PHYSICAL REVIEW C VOLUME 5, NUMBER 3 MARCH 1972

Sub-Coulomb Transfer Reactions on Actinide Nuclei*

J. R. Erskine
Argonne National Laboratory, Argonne, Illinois 60439
(Received 28 October 1971)

Surprisingly large discrepancies have been found between some measured and calculated cross sections for sub-Coulomb transfer reactions on several actinide nuclei. The calculated cross sections of strongly excited states with $J \geq \frac{7}{2}$ are generally too small by a factor of 2–3, such as Siemssen and Erskine had observed in the reaction ^{182}W$(d,p)^{183}$W. A few exceptions to the above rule are found for weakly excited states. In the present study, the use of very low bombarding energies results in an important simplification of the analysis in that the calculated cross sections then are insensitive to uncertainties in the optical-model parameters. The present results suggest that the discrepancy in cross sections probably results from inadequate treatment of the asymptotic tail of the bound-state wave function rather than from neglect of inelastic scattering processes in the incoming and outgoing waves.

I. INTRODUCTION

The single-nucleon transfer reactions (d, p), (d, t), $(^3\text{He}, d)$, and $(^3\text{He}, \alpha)$ have been used for some time to study single-particle excitations in heavy deformed nuclei.[1-6] The usual procedure has been to bombard even-even target nuclei in the rare-earth or actinide region and to measure the differential cross sections for transitions to the various members of the rotational band built on the single-particle excitation. Many single-particle states have been identified by this technique. The extensive mapping which has taken place[7,8] has been made possible by the fact that the relative cross sections of the transitions to the different members in the rotational band qualitatively agree with calculations that use simple Nilsson wave functions for the deformed orbitals and the distorted-wave Born approximation (DWBA) for the reaction mechanism.

However, a number of serious discrepancies have been found in the relative differential cross sections for some transitions – especially for the weak transitions. These discrepancies frequently have been explained by broad statements which suggest either that the Nilsson model is too simple a description to explain such fine details or that a neglected feature of the reaction mechanism causes these observed discrepancies. However, no detailed explanation nor cure for these discrepancies has yet been found.

A different and probably related problem, first found by Siemssen and Erskine[9] and later verified by Gastebois, Fernandez, and Laget[10], is that at 12-MeV bombarding energy in (d, p) reactions on rare-earth nuclei, the measured absolute cross sections were about twice those obtained in calculations that assumed the Nilsson single-particle model and used conventional distorted-wave (DW) calculations. This discrepancy in the absolute cross section occurs if the optical-model parameters used in the DW calculations are those that fit angular distributions for the elastic scattering of the particles involved in both the incoming and outgoing channels. The fact that the same discrepancy was found with the reaction[11] ^{182}W$(t, d)^{183}$W indicates that the result does not depend on the choice of particles used in the entrance or exit channels. The fact that the same discrepancy occurs for two different reactions suggests that the treatment of the bound-state wave function in the DW analysis might be the source of the difficultly. This difficulty in the absolute cross section is frequently avoided by choosing a somewhat arbitrary set of optical-model parameters that gives good single-particle cross sections but does not fit the elastic scattering data.

One possible explanation for the above difficulties is that inelastic scattering effects on the incoming and outgoing channels must be taken into account in the reaction process. One of the earliest of the many theoretical studies of this problem was the work of Penny and Satchler,[12] who showed how the DW theory of direct reactions could be modified so that the DW's would include the effects of strong inelastic scattering. To carry out this program requires a formidable computational effort. Braunschweig, Tamura, and Udagawa[13] report nonadiabatic coupled-channel calculations which solve this problem exactly for the reaction ^{24}Mg$(d, p)^{25}$Mg. However, much computer time is needed to do cases involving heavy deformed nuclei. Iano and Austern[14] and Iano, Penny, and Drisko[15] made a number of simplifying assumptions, the most important of which is the adiabatic approximation, in order to calculate the effects of elastic scattering. Kunz, Rost, and Johnson[16] describe a further simplification of the

Iano-Austern theory, in which the only change from the usual DW procedure is a simple modification of the optical-model potentials for the incoming and outgoing waves. Ascuitto and Glendenning[17] have described a procedure, equivalent to the Penny-Satchler calculation, which uses the coupled-channel source-term method. Recently Glendenning and Mackintosh[18,19] published calculations of the effects of inelastic scattering processes on (d, p) reactions on the light rare-earth nuclei. To date, the results of all these efforts to calculate the effects of the inelastic scattering process show that the changes in the transfer cross sections are typically 10–20% for the strongest transitions in the spectrum. For the weak transitions the calculations predict much larger changes which tend to improve the agreement between the theory and the limited data now available. However, since inelastic scattering contributions seem to produce only small changes in cross section for strong transitions, it seems unlikely that this approach would increase the cross section by the factor of 1.5–2 needed to explain the finding of Siemssen and Erskine.

The present experiment was started in order to shed more light on the above difficulties. The basic idea was to use the Coulomb stripping and pickup reactions to eliminate the ambiguities in the optical-model parameters as well as (hopefully) the need for complicated coupled-channel calculations for incoming and outgoing waves.

The Coulomb stripping reaction was first shown to be a powerful tool for nuclear spectroscopy in the study of the reaction ^{209}Bi$(d, p)^{210}$Bi by Erskine, Buechner, and Enge.[20] At low bombarding energies (7–8 MeV) the reaction mechanism is especially simple, since the transfer process takes place far outside (12–20 fm) the nuclear surface, where the incoming and outgoing waves are relatively insensitive to distortions caused by the nuclear potential. The reaction mechanism is simple, and closed-form expressions for the cross sections and angular distributions have been obtained by Lemmer.[21] Dost and Hering[22] found that the absolute cross sections calculated with a DW theory that used a Woods-Saxon bound-state potential were in good agreement with theoretical expectations for the case of the reaction ^{208}Pb$(d, p)^{209}$Pb. Similar results were found by Dost, Hering, and Smith[23] and Jeans *et al.*[24] Körner and Schiffer[25] have turned this observation around and have made the assumption that the spectroscopic factor in Coulomb pickup reactions for particular energy levels in lead are unity. Then measured cross sections could be used to determine the parameters of the bound-state wave function. The parameters found are generally consistent with what has been measured by other techniques, although the values of r_0 and a tend to be slightly different ($r_0 \approx 1.21$ fm, $a = 0.8$ fm). With reasonable success for the reactions ^{208}Pb$(d, p)^{209}$Pb and ^{208}Pb$(d, t)^{207}$Pb, one would hope that Coulomb stripping and pickup reactions would be valuable in clarifying the situation for single-nucleon transfer reactions on heavy deformed nuclei.

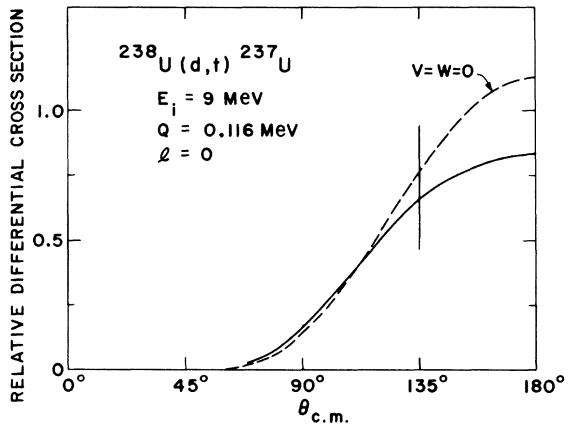

FIG. 1. Typical angular distribution of a Coulomb pickup reaction. Two DW calculations are shown for the reaction ^{238}U$(d, t)^{237}$U at 9 MeV. In the calculation shown by the dashed curve, the optical-model potentials were set to zero to demonstrate the relative lack of sensitivity of the cross section to the optical-model parameters.

II. THEORY

A. Sub-Coulomb Transfer Reactions

For the Coulomb stripping or Coulomb pickup process to occur, the kinetic energies of both the incoming and outgoing particles in the reaction must be so low that the Coulomb potential keeps the particles from getting close to the nucleus. When these conditions are met, the angular distribution of the reaction has the characteristic backward-angle peak shown in Fig. 1, in which the curves were calculated with the program JULIE[26] which evaluates the cross section with the DWBA.[27] The incoming and outgoing particles will inevitably interact slightly with the nuclear potential in most situations in which Coulomb transfer reactions are studied, since the cross section would be too small to measure otherwise. However, the most important advantage of the Coulomb transfer reactions is that the nuclear part of the interaction contributes only a small fraction of the cross section and therefore lack of knowledge of this nuclear part introduces negligible uncertainty in the cross section. This point is illustrated in Fig. 1, which shows angular distributions calcu-

lated with and without nuclear optical-model potentials. At 135° the cross section changes by about 15% when the nuclear potentials are set to zero. This is the worst case, since the use of even roughly estimated values of the optical-model potentials will considerably reduce this kind of uncertainty in the calculations.

It is interesting to use the DW code to calculate at what distance from the nucleus most of the contribution to the cross section arises. Figures 2 and 3 show the contribution to the differential cross section at 135° as a function of the radius for the (d, p) and (d, t) reactions on uranium at 9- and 12-MeV bombarding energy. From the figures, it is obvious that the cross section depends strongly on the amplitude of the asymptotic tail of the bound-state wave function and very little on the amplitude of the wave function inside the nucleus. This is especially true for the reactions at 9-MeV bombarding energy. Even at 12 MeV, most of the cross section arises at distances beyond the nuclear surface.

B. Spectroscopic Factors

It is customary to assume that the expression for the differential cross section may be factored into a part that describes the reaction mechanism and a part that depends on the internal structure of the nuclear levels involved. This assumption usually leads to a basic inconsistency which is slurred over in the usual calculation of cross sections on deformed nuclei. More will be said about this in Sec. II D. However, when the reaction mechanism is assumed to be separable from the nuclear structure, then the expression for the differential cross section of a (d, p) or (d, t) reaction on a spin-0 target is

$$d\sigma/d\Omega = (2J+1)S_J\theta_J^{\mathrm{DW}}, \tag{1}$$

where J is the spin of the final state, θ_J^{DW} is the intrinsic single-particle cross section usually obtained from DW calculations of the reaction mechanism, and S_J is the spectroscopic factor which contains information about internal nuclear structure. For single-nucleon transfer reactions on deformed spin-0 target nuclei, the spectroscopic factor is usually written[9,28]

$$S_J^{\kappa} = [2/(2J+1)](C_J^{\kappa})^2 P_{\kappa}, \tag{2}$$

where κ denotes the specific state being populated, P_{κ} is the pairing factor (to be described below) for

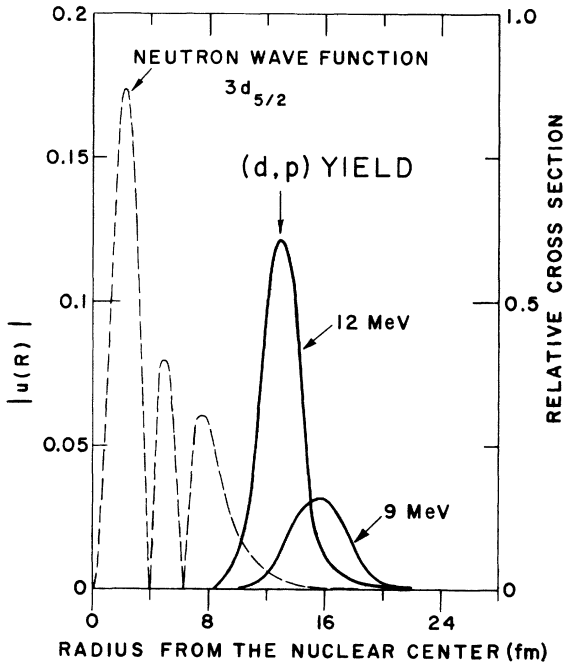

FIG. 2. Spatial origin of the differential cross section in the reaction $^{238}U(d, p)^{239}U$ to the ground state at 135°. The curves were calculated with a DW code by changing the lower-cutoff radius in small steps. The results are shown for two bombarding energies (9 and 12 MeV). At 9 MeV most of the cross section originates far out on the tail of the neutron wave function.

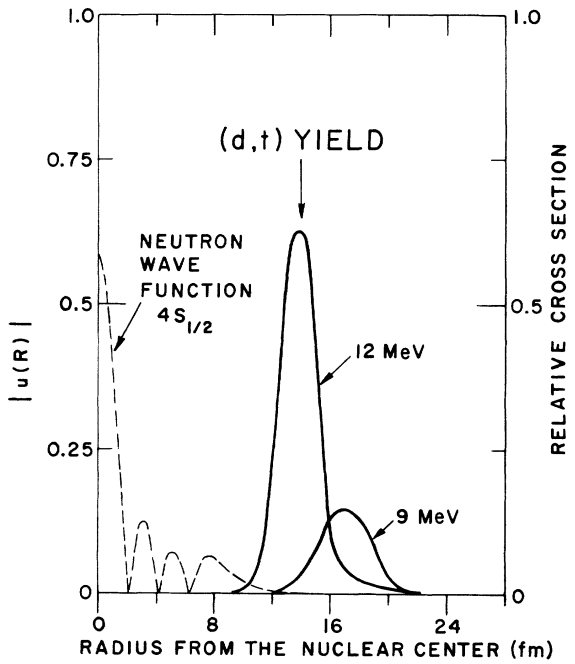

FIG. 3. Spatial origin of the differential cross section in the reaction $^{238}U(d, t)^{237}U$ to the ground state at 135°. The curves were calculated with a DW code by changing the lower-cutoff radius in small steps. The results are shown for two bombarding energies (9 and 12 MeV). At 9 MeV most of the cross section originates far out on the tail of the neutron wave function.

that state in the target, and C_J^κ is an expansion coefficient in the expression for the deformed single-particle wave function.[29] These wave functions are usually written as

$$\chi^\kappa = \sum_J C_J^\kappa \phi_{Jl} , \tag{3}$$

where for the case of Nilsson wave functions[29] the basis wave functions ϕ_{Jl} of the expansion are spherical oscillator wave functions.

Many calculations of deformed single-particle wave functions have been reported,[29-32] each with a somewhat different type of central potential. Several of these calculations for the $\frac{1}{2}^+[631]$ orbital, all with deformation parameter $\beta_2 = 0.23$, are compared in Table I. The Nilsson wave functions[29] are computed with $\mu = 0.45$ and $\kappa = 0.05$. Chasman[32] used a Woods-Saxon potential with momentum dependence to improve the behavior of tightly bound states, which are poorly described by a simple Woods-Saxon potential. Gareev, Ivanova, and Shirikova[31] do a Woods-Saxon calculation with higher-order deformations added; their wave functions given are for $\beta_4 = 0.08$. The differences between the three sets of C_J are minor except for the small components, which sometimes differ by more than a factor of 2.

The pairing factor P_κ in Eq. (2) describes the overlap between the pairing parts of the wave functions of the target and final state. For the (d, p) reaction on an even-even target, this factor can be written exactly as[33]

$$P_\kappa = \langle \phi_\kappa (A+1) | a_\kappa^\dagger | \phi_0(A) \rangle^2 , \tag{4}$$

where ϕ_κ indicates the state in the final nucleus in which the single-particle level κ is blocked, and $\phi_0(A)$ designates the wave function of the A-nucleon target. The overlap integral is complicated to compute, since one needs complete pairing wave functions for the target and for each final state required. A good approximation to the exact calculation is

$$P_\kappa \approx 1 - \langle N_\kappa(A) \rangle , \tag{5}$$

where $\langle N_\kappa(A) \rangle$ is the occupation probability for level κ in the target nucleus. For a (d, t) reaction, $P_\kappa \approx \langle N_\kappa(A) \rangle$.

In the present work, pairing factors were computed with BCS pairing theory. In this case $P_\kappa \approx 1 - \langle N_\kappa(A) \rangle = U_\kappa^2$ for (d, p) reactions, where U_κ is the pairing emptiness factor computed for level κ in the even-even system. The particular technique used to compute the BCS pairing overlap factors was as follows. The single-particle energies used were those that Braid *et al.*[33] extracted from measured excitation energies in ^{235}U by the exact method of Chasman.[34] The pairing gap parameter Δ was varied until the excitation energies in ^{235}U calculated with BCS theory agreed with measured energies. The value $\Delta = 0.6$ MeV was found to give the best fit to the experimental energies. The excitation energies E_x were evaluated by doing a series of BCS calculations with particular states blocked. Excitation energies were not calculated from differences in quasiparticle energies as is sometimes done. Rather, excitation energies were calculated from the formula

$$E_x = E_{\mathrm{BCS}}^\kappa + E_{\mathrm{SP}}^\kappa + E_0 , \tag{6}$$

where E_{BCS}^κ is the BCS total energy with level κ blocked, E_{SP}^κ is the single-particle energy of level κ, and E_0 is a constant. The size of the errors arising from the use of this method was checked by comparing a few overlap factors computed exactly from good pairing wave functions[34] with the pairing factors evaluated with BCS. For those cases of interest in the present study, the BCS pairing factors were within 10% of those computed with the more exact procedure. Finally BCS calculations for both ^{232}Th and ^{238}U were done with $\Delta = 0.6$ MeV. These calculations of pairing factors for (d, p) and (d, t) reactions on ^{232}Th and ^{238}U were made with the assumption that the single-particle energies are the same for all these nuclei.

TABLE I. Comparison of deformed single-particle wave functions for the $\frac{1}{2}^+[631]$ orbital, all with deformation parameter $\beta_2 = 0.23$.

J	C_J^2 Chasman (Ref. 32)	C_J^2 Nilsson (Ref. 29)	C_J^2 Gareev *et al.* (Ref. 31)
$\frac{1}{2}$	0.147	0.133	0.141
$\frac{3}{2}$	0.326	0.300	0.270
$\frac{5}{2}$	0.011	0.037	0.028
$\frac{7}{2}$	0.056	0.118	0.041
$\frac{9}{2}$	0.217	0.190	0.262
$\frac{11}{2}$	0.211	0.200	0.182
$\frac{13}{2}$	0.032	0.022	0.010

C. DW Calculations

DW calculations were performed with program JULIE[26] coded for an IBM 360/75 computer. To ensure consistency with previous work, test calculations were compared with the DW results reported in the Coulomb stripping studies of Jeans *et al.*[24] and Dost, Hering, and Smith.[23]

The general approach was to do DW calculations for the (d, p) and (d, t) reactions with the same neutron-potential parameters that Jeans *et al.*[24] found to give good spectroscopic factors for the reaction ^{208}Pb$(d, p)^{209}$Pb. Consequently, no attempt to do finite-range calculations or to include a correction for nonlocality of the potentials was made. Instead, the procedure was to use zero-range DW calculations that included a spin-orbit term in the bound-state potential. For the reaction ^{208}Pb$(d, p)^{209}$Pb, Jeans *et al.* found that the best fit to the spectroscopic factors was obtained with $r_0 = 1.23$ fm, $a = 0.65$ fm, and $V_{so} = 7$ MeV, with the real well depth adjusted to fit the empirical separation energy. These values for r_0 and a were adopted for all DW calculations. Instead of a fixed V_{so} term, a spin-orbit parameter $\lambda = 26$ was used because of the structure of the code JULIE. This change in the treatment of the spin-orbit term should have only a minor effect on the calculated cross section. Normalization factors of 1.50 and 3.33 were used for (d, p) and (d, t) reactions, respectively.

Körner and Schiffer[25] have recently studied the reaction ^{208}Pb$(d, t)^{207}$Pb at low bombarding energies in order to investigate the parameters of the bound single-hole wave functions. They find that there is considerable ambiguity in the potentials; but if one selects the potential that best reproduces the observed binding and cross sections of the single-hole states ($3p_{1/2}$, $3p_{3/2}$, $2f_{5/2}$, $2f_{7/2}$, and $1i_{13/2}$) in ^{207}Pb, the radial parameters would be about $r_0 = 1.21$ fm and $a = 0.8$ fm. The only requirement on the spin-orbit potential is that it have a radius $r_{so} \leq 0.85 r_0$. This parameter set produces a 10–30% increase in cross section over the parameter set of Jeans *et al.* for the reaction ^{238}U$(d, t)^{237}$U at 9 MeV and 135°. This difference is small compared with the discrepancies between observed and calculated spectroscopic factors for the (d, t) reactions in the present study. Consequently, to keep things simple the same neutron well parameters, those of Jeans *et al.*, were used in both the (d, p) and (d, t) calculations.

Measurement of optical-model parameters at the low bombarding energies and with the heavy nuclei used in this experiment is difficult or impossible because there is so little structure in the elastic scattering angular distributions. Consequently, the parameters chosen are extrapolations from elastic scattering data taken either at higher bombarding energies or with lighter nuclei. This procedure ignores inelastic scattering effects, which become especially important for deformed nuclei.

The optical-model parameters used in the DW calculations are given in Table II. The deuteron parameters are those used by Liers *et al.*[35] and come from an analysis of data taken with 11.8-MeV deuterons scattered from ^{208}Pb. The proton parameters are due to Macefield and Middleton,[36] who used them to fit angular-distribution data from the reaction ^{238}U$(d, p)^{239}$U at 12 MeV. The triton parameters are those found by Becchetti and Greenlees,[37] who simultaneously fitted a large amount of data on elastic scattering of tritons. Many other sets of optical-model parameters were tried. None of these gave appreciably different cross sections at the lowest bombarding energy used in the present experiment. At 12 MeV, however, the cross sections calculated from different optical-model sets differed by more than a factor of 2.

D. Inconsistencies

The common prescription for calculating cross sections for transfer reactions on deformed nuclei contains a well-known inconsistency which is usually ignored because the prescription has appeared to work so well. The difficulty is that the set of spherical wave functions which form the basis upon which the deformed single-particle wave function is expanded is usually not at all the same as the bound-state wave function used in the DW calculation. For example, harmonic-oscillator functions are the basis set for Nilsson wave functions, yet the DW codes normally use a Woods-Saxon potential for the bound state with the additional special feature that the well depth is empirically adjusted to fit the measured separation energy.

The surprising thing is that this inconsistent use of spherical wave functions works at all. The violence done is especially obvious when states deep

TABLE II. Optical-model parameters used in the DW calculations. The notation is that of Becchetti and Greenlees (Ref. 37).

Particle	V_R (MeV)	r_R (fm)	a_R (fm)	W_V (MeV)	W_{SF} (MeV)	r_I (fm)	a_I (fm)	r_c (fm)
d	109.9	1.063	1.038	9.8	0	1.501	0.728	1.25
p	57	1.30	0.5	8	0	1.30	0.50	1.30
t	161.4	1.20	0.72	0	17.08	1.40	0.86	1.25

TABLE III. ^{231}Th levels studied in this work. Their excitation energies, spin-parities, and orbital identifications are given. The experimental and calculated spectroscopic factors are listed together with the P_κ and C_J^2 used. The measured values for the reduced normalization factors Λ_{expt} are also given.

E_x (keV)	J^π	Orbital	P_κ	C_J^2	S_{calc}	S_{expt}	Λ_{expt}
0	$\frac{5}{2}^+$	$\frac{5}{2}^+[633]$	0.75	0.023	0.0049 [a]	0.000 87 ± 0.000 18	0.48 ± 0.10
42	$\frac{7}{2}^+$	$\frac{5}{2}^+[633]$	0.75	0.144	0.028 [a]	0.027 ± 0.004	0.83 ± 0.12
98	$\frac{9}{2}^+$	$\frac{5}{2}^+[633]$	0.75	0.132	0.015 [a]	0.0082 ± 0.0012	0.26 ± 0.04
164	$\frac{11}{2}^+$	$\frac{5}{2}^+[633]$	0.75	0.657	0.092 [a]	0.108 ± 0.014	0.037 ± 0.005
242	$\frac{5}{2}^+$	$\frac{3}{2}^+[631]$	0.80	0.182	0.049	0.072 ± 0.008	47. ± 5.
324	$\frac{9}{2}^+$	$\frac{3}{2}^+[631]$	0.80	0.461	0.092 [a]	0.196 ± 0.016	7.53 ± 0.6
557	$\frac{1}{2}^+$	$\frac{1}{2}^-[501]$	0.88	0.630	0.55	0.409 ± 0.035	582. ± 50.

[a] Coriolis effects have been included.

in the potential well used for the deformed potential are forced to have wrong energies by the DW procedure. Such energy shifts should cause large changes in the asymptotic tails of the bound-state wave functions, and these changes would drastically alter the cross section. Austern[38] and Prakash and Austern[39] have discussed this problem.

The effects of the above deficiency can be reduced if the DW calculation is performed with a deformed bound-state wave function in which all of the components of different j and l have radial tails corresponding to the correct binding energy. A calculation such as Rost's coupled-channel calculation[40] for a deformed single-particle wave function is presumably needed.

E. Coriolis Mixing

Coriolis mixing can make significant changes in the spectroscopic factors and cross sections if conditions are right. Coriolis effects in each of the nuclei studied were investigated through the use of the code BANDFIT.[41] This code is a search program which fits measured excitation energies on the basis of the single-particle rotational model with Coriolis mixing. The search parameters used were the moments of inertia, band-head energies, decoupling parameters, and sometimes Coriolis matrix elements. After good fits were achieved, spectroscopic factors were calculated with and without Coriolis mixing.

This technique will give only estimates of the amount of mixing, since, as a result of uncertainties in experimental data and deficiencies in the theoretical model, the fits achieved were not always unique. Highly accurate calculations of Coriolis effects are not needed, since in all important cases the changes introduced are small. For the levels studied in this work in ^{233}Th and in ^{237}U, the largest change in spectroscopic factor was 3%. In ^{239}U, Coriolis effects reduced the spectroscopic factor of the $J = \frac{9}{2}$ level of the $\frac{5}{2}^+[622]$ band by 17%.

TABLE IV. ^{233}Th levels studied in this work. Their excitation energies, spin-parities, and orbital identifications are given. The experimental and calculated spectroscopic factors are listed together with the P_κ and C_J^2 used. The measured values for the reduced normalization factors Λ_{expt} are also given.

E_x (keV)	J^π	Orbital	P_κ	C_J^2	S_{calc}	S_{expt}	Λ_{expt}
0	$\frac{1}{2}^+$	$\frac{1}{2}^+[631]$	0.76	0.147	0.112	0.060 ± 0.009	41.8 ± 6.3
17	$\frac{3}{2}^+$	$\frac{1}{2}^+[631]$	0.76	0.326	0.124	0.129 ± 0.010	21.6 ± 1.7
55	$\frac{5}{2}^+$	$\frac{1}{2}^+[631]$	0.76	0.011	0.0028	0.0031 ± 0.0010	0.51 ± 0.17
94	$\frac{7}{2}^+$	$\frac{1}{2}^+[631]$	0.76	0.056	0.011	0.033 ± 0.006	0.20 ± 0.04
107	$\frac{9}{2}^+$	$\frac{5}{2}^+[622]$	0.83	0.654	0.108	0.155 ± 0.015	0.92 ± 0.09
159	$\frac{9}{2}^+$	$\frac{1}{2}^+[631]$	0.76	0.217	0.033	0.060 ± 0.007	0.34 ± 0.04
252	$\frac{15}{2}^-$	$\frac{7}{2}^-[743]$	0.76	0.905	0.086	0.178 ± 0.030	0.000 41 ± 0.000 07
326	$\frac{9}{2}^+$	$\frac{5}{2}^+[633]$	...	...	...	0.104 ± 0.010	0.49 ± 0.05

For the weak transitions to the $\frac{5}{2}^+[633]$ band in ^{231}Th, Coriolis effects decreased the spectroscopic factor of the $J=\frac{9}{2}$ level by 23% and caused smaller changes for all other levels. The results of these calculations for ^{239}U and ^{231}Th have been included in Tables III and VI below.

III. EXPERIMENTAL PROCEDURE

An Enge split-pole magnetic spectrograph[42] was used to record the data. The deuteron beam was furnished by the FN tandem accelerator of the Argonne Physics Division. The relatively large solid angle (3.2 msr) of this spectrograph together with its high resolving power made the present experiment feasible, since one needs to measure small cross sections and levels that are closely spaced in energy. Nuclear emulsions were used to record the spectra. The plates were scanned by the Argonne automatic nuclear-emulsion scanner,[43] and the accuracy of these machine results was checked occasionally by hand scanning. The targets were prepared by evaporating natural thorium and fully depleted uranium from a tantalum boat onto 20–30-μg/cm^2 carbon substrates. A small amount of tantalum was present on the uranium target but this usually did not interfere with the measurements.

For most of the runs, the (d, p) and (d, t) data from one target nucleus were recorded simultaneously. This was made possible by the large momentum range of the split-pole spectrograph. The uranium and thorium data were taken under the identical experimental conditions so that the solid angles were the same for all four reactions studied. The absolute cross sections for the transfer reactions were measured relative to the elastic scattering cross section of the deuteron beam on uranium or thorium. The elastic scattering cross sections at the lowest bombarding energies used deviate from Rutherford scattering by only a few percent. For the 12-MeV data, a measured[44] ratio of 0.70 ± 0.03 for deuteron scattering on uranium at 90° was used. At the intermediate energies, the ratio to Rutherford was calculated with an optical-model code. Elastically scattered deuterons were recorded by a silicon monitor detector at 90°.

The solid angles of the spectrograph and the monitor detector were measured carefully in order to reduce the errors in these solid angles to less than 2%. The principal source of error in the cross section then becomes the statistical fluctuations in the number of counts recorded.

Most of the spectra obtained were fitted with program AUTOFIT.[45] Numerous hand checks were made to understand any errors that might have been introduced. For the case of the reaction ^{238}U$(d, t)^{237}$U, all the data were hand-counted and hand-analyzed to minimize error.

IV. EXPERIMENTAL RESULTS

Typical spectra for the four reactions studied are presented in Figs. 4 and 5. Yield curves for the 29 levels investigated with the (d, p) and (d, t) reactions on ^{238}U and ^{232}Th are shown in Figs. 6–9,

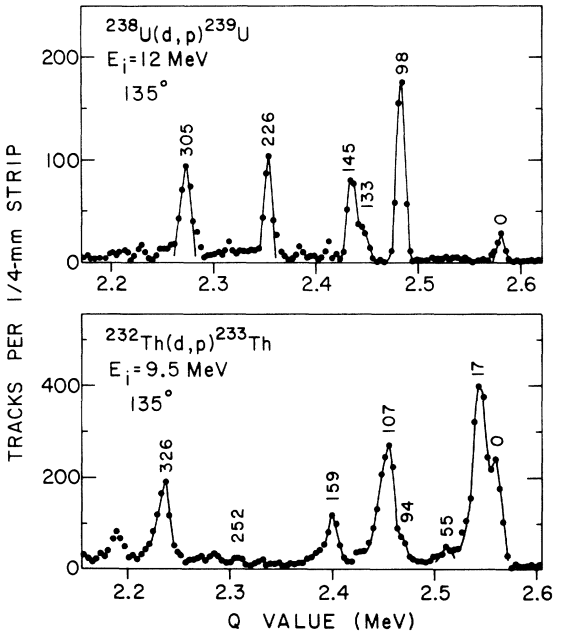

FIG. 4. Typical spectra for (d, p) reactions on targets of ^{238}U and ^{232}Th. The levels studied in the present work are indicated by their excitation energies in keV.

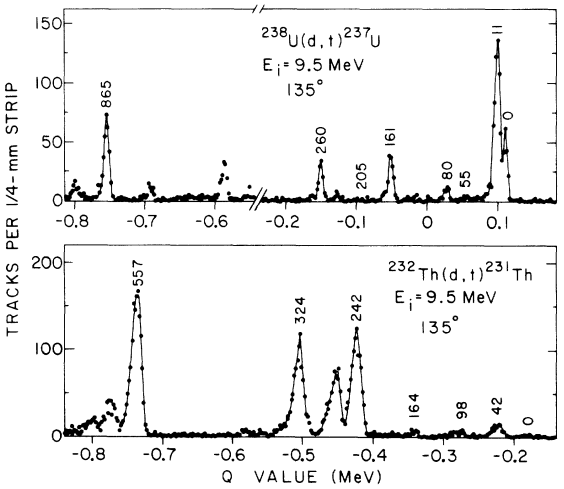

FIG. 5. Typical spectra for (d, t) reactions on targets of ^{238}U and ^{232}Th. The levels studied in the present work are indicated by their excitation energies in keV.

in which absolute differential cross sections are plotted against the bombarding energy. The estimated uncertainty in each datum point is shown by the error bars in the figures. Also shown in each figure are yield curves calculated with the DW code. Details of these calculations appeared in Sec. II C.

V. SUMMARY OF SPECTROSCOPIC INFORMATION

This section is a collection of the available spectroscopic information that is pertinent to the identification of the levels observed in the present study and to the calculation of spectroscopic factors.

The low-lying energy levels of ^{231}Th are known from studies of the α decay[46] of ^{235}U and of the (d, p), (d, t), and (^{3}He, α) reactions.[47-49] The seven well-identified levels studied in the present work belong to the $\frac{5}{2}^+[633]$, $\frac{3}{2}^+[631]$, and $\frac{1}{2}^-[501]$ bands. These states are listed in Table III together with calculated spectroscopic factors for the (d, t) reaction.

The most complete study of the low-lying levels of ^{233}Th is the work of von Egidy *et al.*,[50] who used data from the (d, p) reaction and on both high- and low-energy γ rays following neutron capture in ^{232}Th. Seven single-particle states were identified. The present experiment treats data from eight levels belonging to the lowest three bands, namely the $\frac{1}{2}^+[631]$, $\frac{5}{2}^+[622]$, and $\frac{7}{2}^-[743]$. Spectroscopic details of the levels investigated in ^{233}Th are given in Table IV.

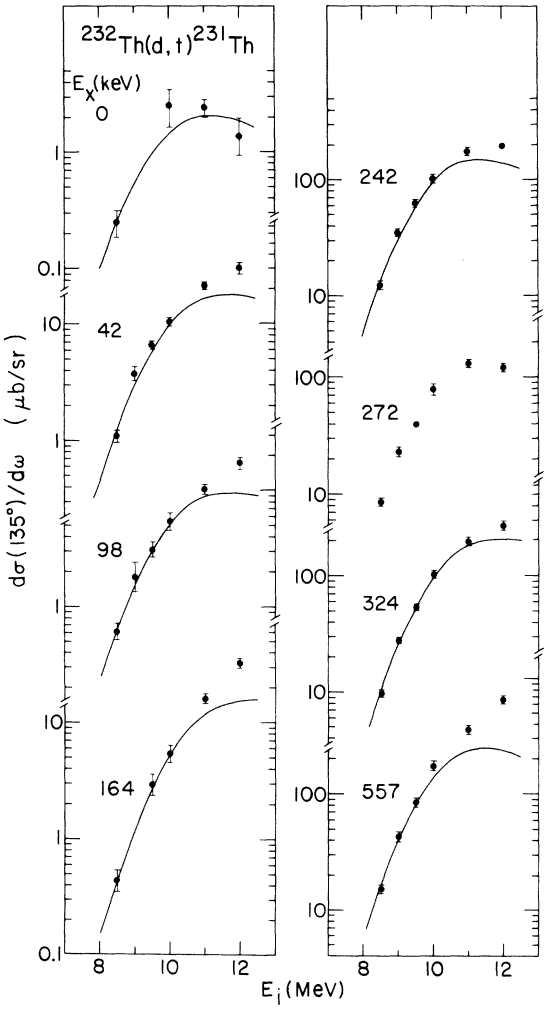

FIG. 6. Measured yield at 135° for the reaction ^{232}Th-$(d, t)^{231}$Th to the indicated levels, plotted as a function of bombarding energy. The curves were calculated with the distorted-wave theory.

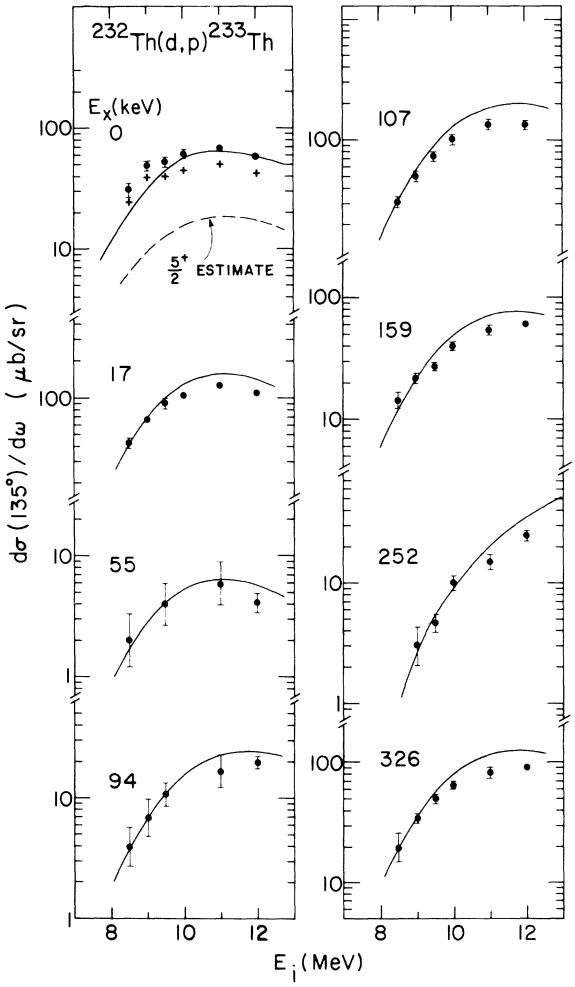

FIG. 7. Measured yield at 135° for the reaction ^{232}Th-$(d, p)^{233}$Th to the indicated levels, plotted as a function of bombarding energy. The curves were calculated with the distorted-wave theory.

The low-lying levels in ^{237}U have been investigated[47-49,51] with the (d, p), (d, t), and (^{3}He, α) reactions as well as by α and β decay studies.[46] The ground-state band is built on the $\frac{1}{2}^+[631]$ state. As indicated in Table V, six members of this band were observed in the present study. Unfortunately, the $I = \frac{9}{2}$ level at 161 keV lies within a few keV of the $I = \frac{5}{2}$ level of the $\frac{5}{2}^+[622]$ state. This circumstance added uncertainty in the cross section of the $I = \frac{9}{2}$ level, since the contribution of the $I = \frac{5}{2}$ level to the cross section of the doublet had to be estimated from its yield in the $\frac{5}{2}^+[622]$ rotational band observed[33] in the reaction ^{236}U(d, t)-^{235}U. The $I = \frac{9}{2}$ level of the $\frac{5}{2}^+[622]$ state is clearly observed. The level at 865 keV is predominantly the $I = \frac{1}{2}$ level from the $\frac{1}{2}^-[501]$ state.

The reaction ^{238}U$(d, p)^{239}$U has been used by Macefield and Middleton,[36] by Sheline *et al.*,[52] and by Braid *et al.*[47] to study the level structure of ^{239}U. The reaction ^{238}U$(\bar{n}, \gamma)^{239}$U was used by Bollinger and Thomas[53] to locate several additional bands above 600-keV excitation. The following single-particle states have been found at low excitation: $\frac{5}{2}^+[622]$, $\frac{1}{2}^+[631]$, and $\frac{7}{2}^+[624]$. Five levels from the $\frac{5}{2}^+[622]$ and $\frac{1}{2}^+[631]$ bands were studied. However, the levels from the $\frac{7}{2}^+[624]$ band are quite weak or not clearly isolated from other levels, and consequently poor-quality data resulted for this state. The levels studied in this work are listed in Table VI.

VI. DISCUSSION

A. Yield Curves

The calculated yield curves were matched to the experimental values (Figs. 6–9) by optimizing the fit at the lowest bombarding energy. In all cases, the slope of the calculated curve at low bombarding energy agrees well with the measured points. Only at the highest energies used do the curves disagree significantly in some cases.

The best agreement occurs for the reaction ^{238}U$(d, p)^{239}$U (Fig. 9). This good agreement near 12 MeV may be fortuitous, since the optical-model parameters are not well known. For most of the yield curves for the reaction ^{232}Th$(d, p)^{233}$Th (Fig. 7), the agreement is poorer in spite of the fact that the same optical-model parameters were used to calculate all (d, p) curves. This point is best seen by comparing the fit to the 98-keV level of ^{239}U (Fig. 9) with the fit to the 107-keV level of ^{233}Th (Fig. 7). Both levels have the same l, j,

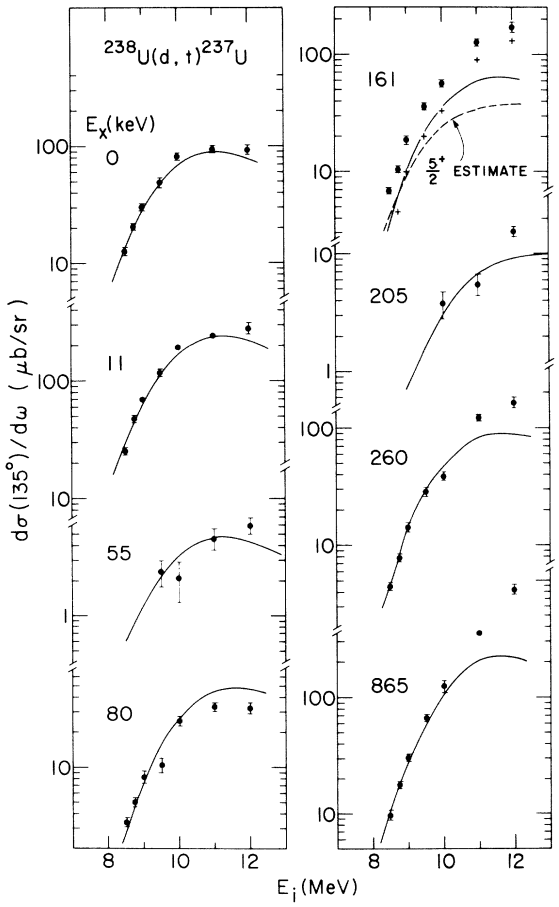

FIG. 8. Measured yield at 135° for the reaction ^{238}U$(d,t)^{237}$U to the indicated levels, plotted as a function of bombarding energy. The curves were calculated with the distorted-wave theory.

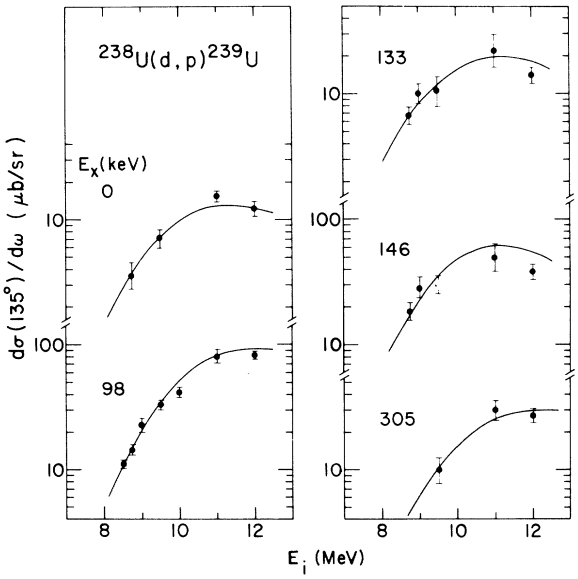

FIG. 9. Measured yield at 135° for the reaction ^{238}U$(d, p)^{239}$U to the indicated levels, plotted as a function of bombarding energy. The curves were calculated with distorted-wave theory.

TABLE V. ^{237}U levels studies in this work. Their excitation energies, spin-parities, and orbital identifications are given. The experimental and calculated spectroscopic factors are listed together with the P_κ and C_J^2 used. The measured values for the reduced normalization factors Λ_{expt} are also given.

E_x (keV)	J^π	Orbital	P_κ	C_J^2	S_{calc}	S_{expt}	Λ_{expt}
0	$\frac{1}{2}^+$	$\frac{1}{2}^+[631]$	0.62	0.147	0.091	0.063 ±0.005	111. ±8.8
11	$\frac{3}{2}^+$	$\frac{1}{2}^+[631]$	0.62	0.326	0.101	0.159 ±0.012	77.6 ±5.9
55	$\frac{5}{2}^+$	$\frac{1}{2}^+[631]$	0.62	0.011	0.0023	0.0018 ±0.0004	0.91 ±0.2
80	$\frac{7}{2}^+$	$\frac{1}{2}^+[631]$	0.62	0.056	0.0087	0.067 ±0.014	1.79 ±0.37
161 [a]	$\frac{9}{2}^+$	$\frac{1}{2}^+[631]$	0.62	0.217	0.027	0.048 ±0.016 [b]	1.37 ±0.46
	$\frac{5}{2}^+$	$\frac{5}{2}^+[622]$	0.49	0.071			
205 [a]	$\frac{11}{2}^+$	$\frac{1}{2}^+[631]$	0.62	0.211	0.022	0.065 ±0.018 [b]	0.019 ±0.005
	$\frac{7}{2}^+$	$\frac{5}{2}^+[622]$	0.49	0.001			
260	$\frac{9}{2}^+$	$\frac{5}{2}^+[622]$	0.49	0.654	0.064	0.071 ±0.004	2.20 ±0.12
865	$\frac{1}{2}^-$	$\frac{1}{2}^-[501]$	0.95	0.630	0.60	0.38 ±0.03	579. ±46.

[a] Assumed doublet.

[b] Contribution from other doublet member has been removed.

and orbital assignment; and yet the calculated curve lies 20–30% above the ^{233}Th data points at 11–12 MeV, whereas for ^{239}U the calculated yield curve fits the data very well. This difference suggests that either the optical-model potentials or inelastic scattering effects or both are different for the two reactions.

The yield curves (Figs. 6 and 8) for the (d, t) reaction on ^{232}Th and ^{238}U exhibit a number of very interesting properties. A j dependence can be seen in the different behavior of the 80- and 260-keV states of ^{237}U (Fig. 8). Both states are $l=4$, but one is $J=\frac{7}{2}$ and the other $J=\frac{9}{2}$ (see Table V). The $J=\frac{7}{2}$ data points (80 keV) fall considerably below the calculated curve at 11–12 MeV, whereas the $J=\frac{9}{2}$ data points (260 keV) lie above the calculated curve at this same energy. The 80- and 260-keV levels belong to different orbitals, but the 80- and 161-keV levels belong to the same orbital, $\frac{1}{2}^+[631]$, and are $J=\frac{7}{2}$ and $\frac{9}{2}$. Unfortunately, the cross section for the reaction to the 161-keV level is somewhat uncertain, since another weaker level, the $J=\frac{5}{2}^+[622]$ state at 163 keV, falls nearly at the same energy. Its cross section can be estimated from its yield in the reaction ^{236}U$(d, t)^{235}$U.[33] When the cross section for the level at 161 keV is corrected for this contribution, the experimental yield curve has almost the same shape as the 260-keV level. This indicates that the j dependence in shape is probably not due to a difference in orbital.

A striking feature of the (d, t) yield curves at

TABLE VI. ^{239}U levels studied in this work. Their excitation energies, spin-parities, and orbital identifications are given. The experimental and calculated spectroscopic factors are listed together with the P_κ and C_J^2 used. The measured values for the reduced normalization factors Λ_{expt} are also given.

E_x (keV)	J^π	Orbital	P_κ	C_J^2	S_{calc}	S_{expt}	Λ_{expt}
0	$\frac{5}{2}^+$	$\frac{5}{2}^+[622]$	0.51	0.071	0.012	0.0067 ±0.0012	1.22 ±0.2
98	$\frac{9}{2}^+$	$\frac{5}{2}^+[622]$	0.51	0.654	0.055 [a]	0.075 ±0.006	0.49 ±0.04
133	$\frac{1}{2}^+$	$\frac{1}{2}^+[631]$	0.38	0.147	0.056	0.017 ±0.003	11.4 ±2.0
146	$\frac{3}{2}^+$	$\frac{1}{2}^+[631]$	0.38	0.326	0.062	0.050 ±0.009	8.1 ±1.5
305	$\frac{9}{2}^+$	$\frac{1}{2}^+[631]$	0.38	0.217	0.017	0.020 ±0.004	0.11 ±0.02

[a] Coriolis effects have been included.

$E_d = 12$ MeV is that the measured $l = 1$ cross sections for the level at 865 keV in ^{237}U and the level at 557 keV in ^{231}Th are 3–4 times the calculated ones. Yet the $l = 0$ and $l = 2$ measured yield curves of the reactions to the ground state and 11-keV level of ^{237}U show good agreement with calculated yield curves.

Another interesting feature is observed in the yield curve (Fig. 6) for the $J = \frac{7}{2}$ level at 42 keV in ^{231}Th. The data points fall considerably above the calculated curve, whereas for the $J = \frac{7}{2}$ level in ^{237}U at 80 keV, the data points fall below the calculated curve (Fig. 8). In other words, the $J = \frac{7}{2}$ and $\frac{9}{2}$ levels at 42 and 98 keV in ^{231}Th do not show a j dependence, whereas the 80- and 260-keV levels and possibly the 80- and 161-keV levels in ^{237}U, also $J = \frac{7}{2}$ and $\frac{9}{2}$, do have this property.

The above discrepancies probably cannot be attributed to uncertainties in the optical-model parameters. Many different sets of optical-model parameters were tried in a series of DW calculations and were found to cause an increase or decrease in the calculated cross section at 12 MeV but not at 8 MeV. As would be expected, it was impossible to simultaneously fit the strikingly different yield curves from the 80- and 260-keV levels in ^{237}U, which are $J = \frac{7}{2}$ and $\frac{9}{2}$. Yet it probably would be possible to empirically find optical-model parameters to simultaneously fit the ^{231}Th data for the $J = \frac{7}{2}$, $\frac{9}{2}$, and $\frac{11}{2}$ levels at 42, 98, and 164 keV, since these curves are so similar.

Another very difficult case would be to fit the $l = 1$ levels at 865 keV in ^{237}U and at 557 keV in ^{231}Th. Optical-model parameters that would fit the 12-MeV points in these $l = 1$ data would give very bad fits to the other curves belonging to the same reaction.

The failure of conventional DW calculations to fit the measured yield curves strongly suggests that additional ingredients in the theory are needed, most likely the ability to treat inelastic scattering effects that accompany the transfer process and/or improvements in the bound-state wave function.

B. Spectroscopic Factors

The spectroscopic factors were extracted from the data by matching the calculated yield curves as well as possible to the data points at the lowest energy. The specific match chosen can be seen in Figs. 6–9. The spectroscopic factors corresponding to each case are given in Tables III–VI. The uncertainty given for each value was estimated from the goodness of the fit to the yield curve at low energy. The spectroscopic factors extracted in this way are compared with calculated spectroscopic factors in Figs. 10–13. The calculated values are taken from Tables III–VI. These comparisons lead to the following observations:

(1) The experimental spectroscopic factors tend to follow the calculated values, although the detailed agreement is not good. For most levels (even the strong ones), the difference is a factor of 2 or more.

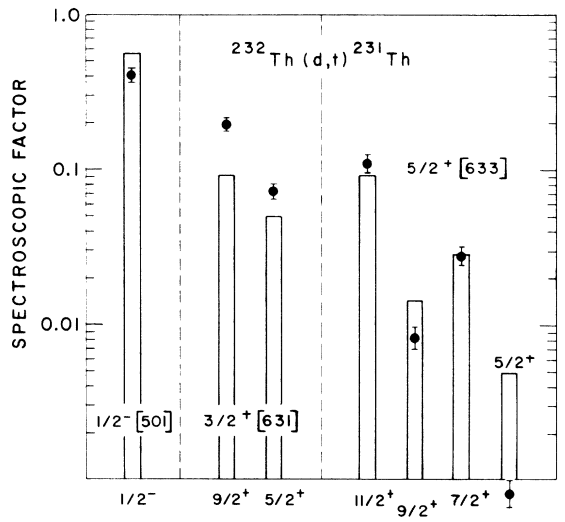

FIG. 10. Comparison of measured and calculated spectroscopic factors for levels observed with the reaction ^{232}Th$(d, t)^{231}$Th. Calculated values are the heights of the bars. The experimental values are the solid circles with associated errors indicated. The orbital identification and J^π for each state are given.

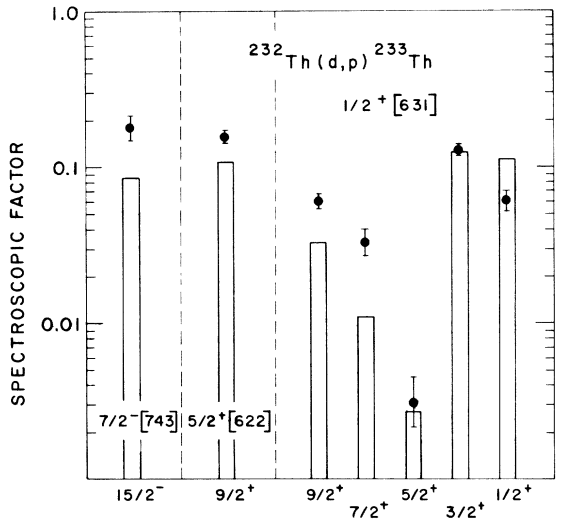

FIG. 11. Comparison of measured and calculated spectroscopic factors for levels observed with the reaction ^{232}Th$(d, p)^{233}$Th. Calculated values are the heights of the bars. The experimental values are the solid circles with associated errors indicated. The orbital identification and J^π for each state are given.

(2) The situation for the $\frac{1}{2}^+[631]$ band is remarkably similar for both the reactions $^{238}U(d, t)^{237}U$ and $^{232}Th(d, p)^{233}Th$. For this band, differences between calculated and measured spectroscopic factors are very similar even though different reactions and nuclei are involved.

(3) The measured spectroscopic factors tend to be larger for the levels with higher J. Most notable are the $J=\frac{7}{2}$, $\frac{9}{2}$, and $\frac{11}{2}$ levels in the $\frac{1}{2}^+[631]$ bands of ^{233}Th and ^{237}U, for which the measured values are 2–8 times the calculated values. An exception occurs for the $J=\frac{9}{2}$ level in the $\frac{5}{2}^+[622]$ band in ^{237}U, for which the measured spectroscopic factor is only 10% larger than the calculated value. Exceptions also occur for the $\frac{5}{2}^+[633]$ band in ^{231}Th. The $J=\frac{7}{2}$ and $\frac{11}{2}$ levels have measured spectroscopic factors which are in good agreement with the calculations but the $J=\frac{9}{2}$ and especially the $J=\frac{5}{2}$ levels are not.

(4) The smallness of the measured spectroscopic factors for the $J=\frac{5}{2}$ level of the $\frac{1}{2}^+[631]$ bands is experimental evidence that inelastic scattering effects in these reactions are probably negligible at low bombarding energy. Nearby levels are strong enough that any appreciable inelastic scattering would probably enhance the cross section for the weak $J=\frac{5}{2}$ level. Of course this argument cannot be conclusive, since inelastic scattering effects are coherent, and hence small yields are not evidence for their absence.

(5) For both ^{231}Th and ^{237}U the extracted spectroscopic factors for the $J=\frac{1}{2}$ level of the $\frac{1}{2}^-[501]$ band are about 30% smaller than the theoretical spectroscopic factors. This is consistent with calculations of Soloviev and Vogel,[54] who predict large phonon admixtures in the wave function of the $\frac{1}{2}^-[501]$ states for these nuclei. Phonon admixtures were not included in the computation of the spectroscopic factors of Tables III–VI.

An illuminating demonstration of the shortcomings of the theoretical analysis used above is to calculate the C_J^2 of the deformed wave function from the extracted spectroscopic factors. Equation (2) can be rearranged to read

$$(C_J^K)^2 = (2J+1)S_J^K/2P_K . \tag{7}$$

The most complete set of spectroscopic factors S_J^K is that for the $\frac{1}{2}^+[631]$ band in ^{237}U. Details of the extraction of the C_J^2 from the data with Eq. (7) are given in Table VII. Theoretical values of C_J^2 from Nilsson wave functions are given for comparison. If the theoretical analysis were adequate, the sum of all the extracted C_J^2 in the band would be unity. However, the sum of the six extracted C_J^2 is 2.07 and would be even greater if the contribution from the $J=\frac{13}{2}$ level were available. If the lower limit given by the estimated error of each spectroscopic factor is used, the sum is

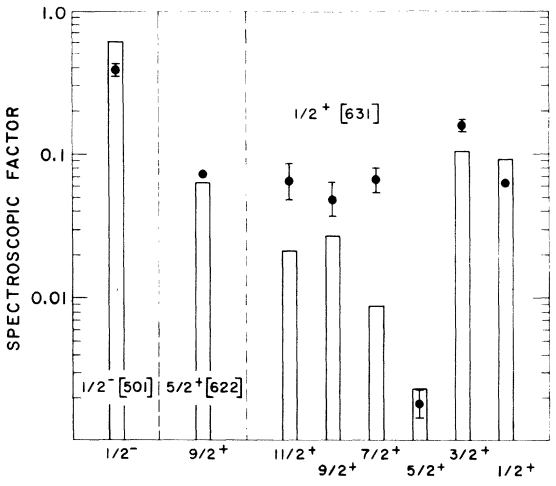

FIG. 12. Comparison of measured and calculated spectroscopic factors for levels observed with the reaction $^{238}U(d, t)^{237}U$. Calculated values are the heights of the bars. The experimental values are the solid circles with associated errors indicated. The orbital identification and J^π for each state are given.

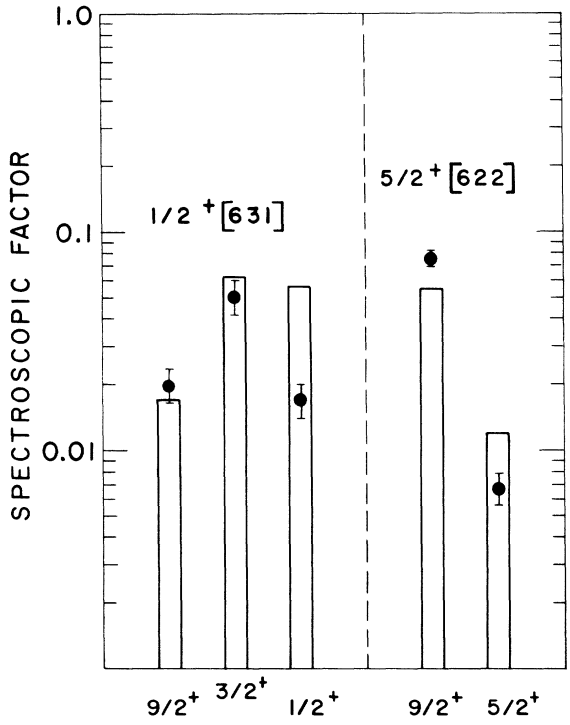

FIG. 13. Comparison of measured and calculated spectroscopic factors for levels observed with the reaction $^{238}U(d, p)^{239}U$. Calculated values are the heights of the bars. The experimental values are the solid circles with associated errors indicated. The orbital identification and J^π for each state are given.

only slightly reduced to 1.8. This kind of analysis clearly shows the inadequacies of the standard DW procedure.

C. Reduced Normalization Factors Λ

In some ways the spectroscopic factor is an unsatisfactory quantity to extract from the cross-section data, since it depends on the particular choice of model for the bound state and particular parameter values for the model. A model-independent quantity which describes the size of the asymptotic tail of the bound-state wave function is the reduced normalization constant Λ defined by Rapaport and Kerman.[55] This quantity is particularly appropriate for sub-Coulomb transfer reactions, since (as is suggested by Figs. 2 and 3) the cross section in the reactions depends only on the size of the asymptotic tail of the neutron wave function and not on the details of the wave function inside the nucleus. No new physics is introduced through the use of the quantity Λ; it is only an attempt to find a better quantity to use in comparing experiment with theory.

The reduced normalization Λ describes the amplitude of the spherical Hankel function which represents the radial part of the neutron bound-state eigenfunction far outside the nucleus. The dimensionless quantity Λ_{lj} is defined through the radial part of the overlap integral between initial and final states, i.e., by the relation

$$\langle f|i\rangle = [(2J+1)\Lambda_{lj}]^{1/2} k^{3/2} h_l^{(1)}(ikr), \qquad r > R_n, \quad (8)$$

where R_n is the nuclear radius and $k=(1/\hbar)(2\mu|B_n|)^{1/2}$, in which μ is the reduced mass of the residual nucleus and B_n is the neutron binding energy.

Reduced normalization factors Λ were extracted from the data with the DW code JULIE and a separate code that calculated Hankel functions. The procedure used was to find the normalization factor N_{lj} of the Hankel function used in the DW code and then modify the extracted spectroscopic factors of Tables III–VI through the use of the relation

$$k^3 \Lambda_{lj} = N_{lj}^2 S_{lj} . \quad (9)$$

The results are also given in Tables III–VI. The values of Λ should be compared with theoretical values calculated from models of deformed nuclear bound states.

TABLE VII. Extraction of C_J^2 components of the deformed wave function for the $\frac{1}{2}^+[631]$ band in ^{237}U. The value $P_\kappa = 0.62$ was used.

E_x (keV)	J	$S_{\text{extracted}}$	C_J^2 Extracted	C_J^2 Nilsson
0	$\frac{1}{2}$	0.063	0.102	0.133
11	$\frac{3}{2}$	0.159	0.513	0.300
55	$\frac{5}{2}$	0.0018	0.009	0.037
80	$\frac{7}{2}$	0.067	0.432	0.118
161	$\frac{9}{2}$	0.048	0.387	0.190
205	$\frac{11}{2}$	0.065	0.629	0.200
			$\sum = 2.07$	

D. Possible Explanation of the Discrepancies

The present experiment provides new data about deformed single-particle wave functions under conditions such that uncertainties in optical-model parameters have negligible effects. However, it is not completely certain that inelastic scattering effects due to Coulomb excitation are really negligible at the lowest bombarding energies employed. From the standard formulas given by the theory of Coulomb excitation,[56] one can calculate the ratio of inelastic to elastic differential cross section to obtain an estimate of the importance of inelastic scattering effects. One finds that for excitation of the lowest 2^+ level by scattering 8.5-MeV deuterons on ^{238}U at 180°, the differential cross section for inelastic scattering is only a few percent of the elastic cross section. On this basis, Coulomb-excitation effects are probably unimportant. Additional but not conclusive evidence is the very small observed cross section of the $J=\frac{5}{2}$ level of the $\frac{1}{2}^+[631]$ band. As mentioned in Sec. VI B, if inelastic scattering effects were important one might expect some of the strength of the $J=\frac{1}{2}$ or $\frac{9}{2}$ level of this band to be shifted to the $J=\frac{5}{2}$ level. Unfortunately the sign of the contribution is not known, and the small cross section may really be due to destructive interference. Nevertheless, it is probably safe to assume that inelastic scattering effects are small at the lowest bombarding energies used in this experiment.

The discrepancies between extracted and calculated spectroscopic factors, shown in Figs. 10–13 and Table III–VI, are most likely due to inadequate treatment of the bound-state wave functions in the analysis, since inelastic scattering effects are probably unimportant. The present experiment is particularly sensitive to the size of the tail of the bound-state wave function and this feature is not what is most desired in the usual calculations of deformed single-particle wave functions. Explanation of the present data may require coupled-channel calculations of the type Rost[40] performed for deformed single-particle wave functions. In the latter calculation, the decay of the tail of each component of the deformed wave function is forced to correspond to the same binding energy. In the usual calculations, this detail is disregarded.

One would expect improvement in the DW calculations if the spherical neutron well could be changed to a deformed well. A crude step in this direction can be made if the DW calculation is done with an increased radius parameter r_0. This procedure is supported by the argument that the mean radius of a deformed nucleus, averaged over many orientations, is somewhat larger than that of a spherical nucleus. Or equivalently, one can increase the diffusivity parameter a. DW calculations were performed to check what effects changes in r_0 and a produced. The results tend to be in the right direction to explain the disagreement in spectroscopic factors (Figs. 10–13). Specifically, for the reaction ^{238}U$(d, t)^{237}$U at 135° and 9 MeV, the neutron well parameter r_0 was increased from 1.23 to 1.35 fm with parameter a held fixed at 0.65 fm. The calculated cross section for $l = 0$ transitions increased by a factor of 1.8 and the cross sections for $l = 6$ transitions increase by the larger factor 3.2. Similar results would have been obtained if a had been increased from 0.65 to 1.0 fm and r_0 held fixed at 1.23 fm. The conclusion is that an increase in the radius or diffuseness of the neutron well tends to give somewhat better agreement with the data, although serious discrepancies still remain.

Another possible explanation for the discrepancies in spectroscopic factors is the calculations should allow proper treatment of the differences between polar and equatorial orbits, i.e., orbits in which the quantum number Ω is small or large. One might expect to observe such effects in the present data, since for reactions where Coulomb effects are strong, it may be important to treat the differences in penetrability of the Coulomb barrier between polar and equatorial orbits. The data on the spectroscopic factors (Figs. 10–13) do not offer much support for the need for this kind of explanation. The trend seems to be that the Ω value of the band does not obviously affect the agreement, although the evidence is quite sparse.

It would be interesting to discover why the usual DW-Nilsson prescription for analysis works so well in some cases. Elbek and Tjom[8] report an analysis of (d, t) data taken at 12 MeV on the $\frac{1}{2}^-[521]$ band in ^{175}Yb. They find very detailed agreement between experiment and theory for the $J = \frac{1}{2}$, $\frac{5}{2}$, and $\frac{7}{2}$ levels. This agreement may be somewhat artificial, since the average optical-model parameters used in their DW analysis do not necessarily fit elastic scattering data, and the analysis did not treat inelastic scattering, which may be sizable at 12-MeV bombarding energy.

Another kind of discrepancy is apparent in most of the yield curves (Figs. 6–9) near 11–12 MeV. At these higher bombarding energies, the failure of the calculated yield curves to follow the data points is probably caused by the neglect of inelastic scattering in the calculation as well as imprecise knowledge of the optical-model parameters. The specific problems mentioned in the discussion of the measured yield curves in Sec. VI A might be solved if the inelastic scattering contributions to the incoming and outgoing waves were properly calculated.

VII. CONCLUSION

Serious inadequacies in the conventional techniques for extracting spectroscopic factors for single-nucleon transfer reactions on deformed heavy nuclei have been demonstrated by this experiment. In particular, this experiment shows that for sub-Coulomb transfer reactions the spectroscopic factors extracted by use of Nilsson wave functions and conventional DW calculation tend to be too large. The size of the discrepancy tends to increase with J, being a factor of 2–3 for $J \geq \frac{7}{2}$. The experimental cross-section data obtained will provide a test of the wave functions of deformed single-particle calculations in which the asymptotic tail has been properly treated. The present cross-section data supplement data on the single-particle energies, and the combined information provides a basis for testing and parametrizing calculations of single-particle states in deformed potentials. Unfortunately, most deformed single-particle calculations to date do not properly treat the asymptotic tail of the bound-state wave function.

ACKNOWLEDGMENTS

The author wishes to thank A. K. Kerman, J. O. Rasmussen, R. R. Chasman, J. P. Schiffer, H. J. Körner, and R. S. Mackintosh for helpful discussions and comments. Many thanks are also due E. Sutter, who gave much competent assistance in analyzing the data.

---

*Work performed under the auspices of the U. S. Atomic Energy Commission.

[1]J. R. Erskine, Phys. Rev. 138, B66 (1965).

[2]M. N. Vergnes and R. K. Sheline, Phys. Rev. 132, 1736 (1963).

[3]D. G. Burke, B. Zeidman, B. Elbek, B. Herskind, and M. C. Olesen, Kgl. Danske Videnskab. Selskab, Mat.-Fys. Medd. 35, No. 2 (1966).

[4]J. Ungrin, D. G. Burke, M. W. Johns, and W. P. Alford, Nucl. Phys. A132, 322 (1969).
[5]M. T. Lu and W. P. Alford, Phys. Rev. C 3, 1243 (1971).
[6]T. W. Elze, T. von Egidy, and J. R. Huizenga, Nucl. Phys. A128, 564 (1969).
[7]M. E. Bunker and C. W. Reich, Rev. Mod. Phys. 43, 348 (1971).
[8]B. Elbek and P. O. Tjom, in *Advances in Nuclear Physics*, edited by M. Baranger and E. Vogt (Plenum, New York, 1969), Vol. III.
[9]R. H. Siemssen and J. R. Erskine, Phys. Rev. 146, 911 (1966); Phys. Rev. Letters 19, 90 (1967).
[10]J. Gastebois, B. Fernandez, and J. M. Laget, Nucl. Phys. A125, 531 (1969).
[11]E. R. Flynn, G. Igo, P. D. Barnes, R. F. Casten, and J. R. Erskine, Nucl. Phys. A159, 598 (1970).
[12]S. K. Penny and G. R. Satchler, Nucl. Phys. 53, 145 (1964).
[13]D. Braunschweig, T. Tamura, and T. Udagawa, Phys. Letters 35B, 273 (1971).
[14]P. J. Iano and N. Austern, Phys. Rev. 151, 853 (1966).
[15]P. J. Iano, S. K. Penny, and R. M. Drisko, Nucl. Phys. A127, 47 (1969).
[16]P. D. Kunz, E. Rost, and R. R. Johnson, Phys. Rev. 177, 1737 (1969).
[17]R. J. Ascuitto and N. K. Glendenning, Phys. Rev. 181, 1396 (1969).
[18]N. K. Glendenning and R. S. Mackintosh, Nucl. Phys. A168, 575 (1971).
[19]R. S. Mackintosh, University of California Lawrence Radiation Laboratory Report No. UCRL-19529, 1970 (unpublished).
[20]J. R. Erskine, W. W. Buechner, and H. A. Enge, Phys. Rev. 128, 720 (1962).
[21]R. H. Lemmer, Nucl. Phys. 39, 680 (1962).
[22]M. Dost and W. R. Hering, Phys. Letters 6, 488 (1965).
[23]M. Dost, W. R. Hering, and W. R. Smith, Nucl. Phys. A93, 357 (1967).
[24]A. F. Jeans, W. Darcey, W. G. Davies, K. N. Jones, and P. K. Smith, Nucl. Phys. A128, 224 (1969).
[25]H. Körner and J. P. Schiffer, unpublished.
[26]R. H. Bassel, R. M. Drisko, and G. R. Satchler, Oak Ridge National Laboratory Report No. ORNL-3240 (unpublished); R. M. Drisko, private communication.
[27]G. R. Satchler, Nucl. Phys. 55, 1 (1964).
[28]G. R. Satchler, Ann. Phys. (N.Y.) 3, 275 (1958).
[29]S. G. Nilsson, Kgl. Danske Videnskab. Selskab, Mat.-Fys. Medd. 29, No. 16 (1955).
[30]A. Faessler and R. K. Sheline, Phys. Rev. 148, 1003 (1966).
[31]F. A. Gareev, S. P. Ivanova, and N. Y. Shirikova, Joint Institute for Nuclear Research, Dubna, Report No. P4-5457, 1970 (unpublished).
[32]R. R. Chasman, Phys. Rev. C 3, 1803 (1971).
[33]T. H. Braid, R. R. Chasman, J. R. Erskine, and A. M. Friedman, Phys. Rev. C 1, 275 (1970).
[34]R. R. Chasman, Phys. Rev. 138, B326 (1965).
[35]H. S. Liers, R. D. Rathmell, S. E. Vigdor, and W. Haeberli, Phys. Rev. Letters 26, 261 (1971).
[36]B. E. F. Macefield and R. Middleton, Nucl. Phys. 59, 631 (1964).
[37]F. D. Becchetti, Jr., and G. W. Greenlees, John H. Williams Laboratory of Nuclear Physics, University of Minnesota, Annual Report, 1969 (unpublished), p. 116.
[38]N. Austern, Phys. Rev. 136, B1743 (1964).
[39]A. Prakash and N. Austern, Ann. Phys. (N.Y.) 51, 418 (1969).
[40]E. Rost, Phys. Rev. 154, 994 (1967).
[41]This code was developed by E. Sutter and the author.
[42]J. E. Spencer and H. A. Enge, Nucl. Instr. Methods 49, 181 (1967).
[43]J. R. Erskine and R. H. Vonderohe, Nucl. Instr. Methods 81, 221 (1970).
[44]N. Williams, private communication.
[45]P. Spink and J. R. Erskine, Argonne National Laboratory Physics Division Informal Report No. PHY-1965B; J. R. Comfort, Argonne National Laboratory Physics Division Informal Report No. PHY-1970B (unpublished).
[46]E. K. Hyde, I. Perlman, and G. T. Seaborg, *The Nuclear Properties of the Heavy Elements* (Prentice-Hall, Englewood Cliffs, New Jersey, 1964), Vol. II.
[47]T. H. Braid, R. R. Chasman, J. R. Erskine, and A. M. Friedman, unpublished.
[48]T. H. Braid, R. R. Chasman, J. R. Erskine, and A. M. Friedman, Phys. Letters 18, 149 (1965).
[49]J. S. Boyno, T. W. Elze, and J. R. Huizenga, Nucl. Phys. A157, 263 (1970).
[50]T. von Egidy, O. W. B. Schult, D. Rabenstein, R. F. Chrien, J. R. Erskine, H. A. Baader, and D. Breitig, unpublished.
[51]T. von Egidy, T. W. Elze, and J. R. Huizenga, Nucl. Phys. A145, 306 (1970).
[52]R. K. Sheline, W. N. Shelton, T. Udagawa, E. T. Jurney, and H. T. Motz, Phys. Rev. 151, 1011 (1966).
[53]L. M. Bollinger and G. E. Thomas, Bull. Am. Phys. Soc. 16, 496 (1971).
[54]V. G. Soloviev and P. Vogel, Nucl. Phys. 92, 449 (1967).
[55]J. Rapaport and A. K. Kerman, Nucl. Phys. A119, 641 (1968).
[56]K. Adler, A. Bohr, T. Huus, B. Mottelson, and A. Winther, Rev. Mod. Phys. 28, 432 (1956).